Conduction Mechanism of Chitosan/Methylcellulose/1-Butyl-3 Methyl Imidazolium Bis (Trifluoromethylsulfonyl) Imide (BMIMTFSI) Biopolymer Electrolyte Doped with Ammonium Triflate

M. S. M. Misenan and A. S. A. Khiar*
Faculty of Science and Technology, Universiti Sains Islam Malaysia (USIM), Bandar Baru Nilai, 71800 Nilai, Negeri Sembilan, Malaysia
*Corresponding author (e-mail: azwanisofia@usim.edu.my)

Chitosan/methylcellulose/1-butyl-3 methyl imidazolium bis (trifluoromethylsulfonyl) imide (BMIMTFSI) biopolymer electrolyte has been prepared via solution casting technique by doping with different weight percentages of ammonium triflate ($NH_4CF_3SO_3$) salt. The films were characterized by impedance spectroscopy to measure the ionic conductivity. Samples with 25 wt.% of $NH_4CF_3SO_3$ exhibited the highest conductivity of 7.64×10^{-4} S cm^{-1} at ambient. Dielectric data showed that the increase in conductivity could be due to the increase in the number of charge carriers, while modulus study confirmed the non-Debye behaviour. Temperature dependence study showed that the polymer electrolyte system obeyed the Arrhenius rule. Conduction mechanism analysis showed that this system matched the Quantum Mechanical Tunnelling (QMT) behaviour. X-ray Diffraction (XRD) spectra, which had been deconvoluted using Origin 8 software disclosed that samples with the lowest degree of crystallinity (X_c %) obtained the highest ionic conductivity. On the other hand, Fourier Transform Infrared (FTIR) spectra, which were also deconvoluted using the same software showed that samples with the highest ionic conductivity had the highest number of mobile ions in this system.

Key words: Polymer electrolyte; polymer blend; ionic liquid; salt

Received: August 2019; Accepted: May 2020

The development of solid polymer electrolyte (SPE) has attracted widespread attention due to its flexibility and ease of preparation into films in large scale [1]. Even though a lot of studies on polymer electrolytes have been completed, most of the studies reported in literature used petrochemical-based polymers, which usually are associated to environmental issues and have high costs. In order to reduce the dependence on petrochemical-based polymers for electrolytes, bio-based polymers may be applied as hosts [2]. In general, SPE should allow a superficial and selective migration of only the desired ions; the best PEs show a high ionic conductivity and transference numbers close to 1.

However, low ionic conductivity of solid biopolymer electrolytes (SBE) usually limits its applications. Therefore, in order to enhance the conductivity of ions in SBE, several methods can be applied such as polymer blending [3-5], co-polymer grafting [5], and addition of plasticizers [7-9] or ceramic [10]. Each of these methods can be applied depending on the materials used. According to Khiar and Arof [11], polymer blending is a well-used technique whenever modification of properties is required because it uses conventional technology at low costs. Many works have been done to blend chitosan with other polymers in order to search for higher conductivity. Table 1 shows some previous reports where chitosan was blended with other polymers and its conductivity.

In the present study, methylcellulose (MC) and chitosan (CS) have been chosen as the host in the polymer electrolyte system. Both MC and CS are biodegradable polymers derived from cellulose and chitin, respectively. In fabricating polymer electrolytes, both are chosen due to the abundance of lone pair electrons present in their backbone which enables the coordination of cations from the added salt [16]. The chemical structures of MC and CS are shown in Figures 1 and 2, respectively.

MC and CS have good polymer blending properties. According to Pinotti *et al*. [17], films formulated with MC, CS, and mixed solutions were homogeneous, transparent, thin, and flexible. Visually, MC films are colorless while CS films have slightly yellowish appearance, where the yellowness shade increases with CS concentration. Besides that, the final properties of MC-CS blend are determined by the miscibility of the polymer that can be formed by intermolecular hydrogen bonds between the polymer components [18].

Table 1. Conductivity of previously studied polymer electrolytes

Polymer Blends	Ionic Conductivity (σ) / Scm^{-1}	References
Methyl Cellulose - Chitosan	1.51×10^{-6}	12
PVA – Chitosan	3.73×10^{-7}	13
Carboxymethyl cellulose – Chitosan	1.21×10^{-5}	14
PEO – Chitosan	3.66×10^{-6}	15

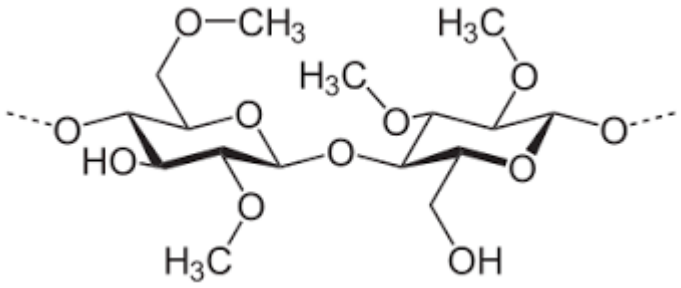

Figure 1. Chemical structure of MC

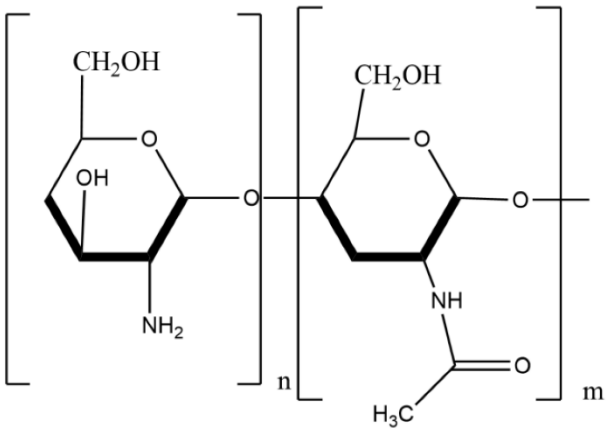

Figure 2. Chemical structure of CS

The main purpose of this research is important to study how the chosen salt has helped to enhance the ionic conductivity of the biopolymer electrolyte membrane, as it would profoundly influence some other parameters such as amorphous nature, ionic conductivity, and electrochemical window stability of the electrolyte. The study of these parameters is vital for electrochemical device applications such as batteries, capacitors, and dye-sensitized solar cells.

MATERIALS AND METHODS

Sample Preparation

Mixtures of MC – CS – 45 wt.% BMIMTFSI doped with various amounts of $NH_4CF_3SO_3$ were prepared by solution casting technique. MC and CS were blended together in 40:60 ratio, in which 0.4 g of methyl cellulose was dissolved in 50 mL distilled water while 0.6 g chitosan was dissolved in 1% diluted acetic acid. 45 wt.% of BMIMTFSI was doped constantly into the polymer blend solution. Then, different amounts of $NH_4CF_3SO_3$ (10 wt.%, 15 wt.%, 20 wt.%, 25 wt.%, 30 wt.%, 35 wt.%, and 40 wt.%) were added into the solution. The solutions were further stirred to form homogenous solutions. Then the solutions were cast into petri dishes and left to dry in a drying cabinet at 25°C and then transferred to a desiccator with silica gel desiccants for further drying to discard any trace of moisture before further analyses. The compositions and labels are tabulated in Table 2.

Table 2. Compositions of biopolymer electrolytes and labels

Ammonium triflate ($NH_4 CF_3 SO_3$), weightage	Label
10	BPEIL SALT 10
15	BPEIL SALT 15
20	BPEIL SALT 20
25	BPEIL SALT 25
30	BPEIL SALT 30
35	BPEIL SALT 35
40	BPEIL SALT 40

Conductivity Measurement

The ionic conductivity study was performed by Impedance Spectroscopy using HIOKI 3531-01 LCR Hi Tester interfaced to a computer at the frequency of 50 Hz - 1 MHz. This study was also carried out at various temperatures in the range of 298 K – 373 K. All the electrolyte films were cut into an equal size of 1 cm in diameter and sandwiched between two stainless steel blocking electrodes under spring pressure. A negative imaginary impedance, Z_i versus real impedance, Z_r graph with the same scale of horizontal and vertical axes was then plotted where the bulk resistance, R_b could be obtained. Hence, the conductivity of the samples at room temperature could be calculated by using the following equation:

$$\sigma = \frac{t}{R_b A} \quad (1)$$

Where R_b is bulk resistance, t is the thickness of the thin film and A is the surface area of contact. In order to measure the thickness of the thin films, a digital micrometer screw gauge was used.

Other recorded data besides impedance $Z(\omega)$ used in impedance spectroscopy are complex permittivity $\varepsilon(\omega)$ and complex dielectric modulus $M(\omega)$. Both the real ε_r and imaginary part ε_i of dielectric constant and electrical modulus can be obtained from the following equations:

$$\varepsilon_r = Z_i/\omega C_o(Z_r^2 + Z_i^2) \quad (2)$$

$$\varepsilon_i = Z_r/\omega C_o(Z_r^2 + Z_i^2) \quad (3)$$

$$M_r = \varepsilon_r/({\varepsilon_r}^2 + {\varepsilon_i}^2) \quad (4)$$

$$M_i = \varepsilon_i/({\varepsilon_r}^2 + {\varepsilon_i}^2) \quad (5)$$

Where $C_o = \varepsilon_o/AT$ and ε_o is the permittivity of the free space.

X-ray Diffraction Analysis

X-ray diffraction (XRD) analysis was carried out using Siemen D5000 X-ray diffractometer. X-rays of the wavelength of 1.5406 Å were generated by a Cu Kα radiation scanned at ambient temperature with the voltage of 30 kV and current source of 15 mA. The samples were positioned on the sample holder of the diffractometer and scanned at 2θ angle from 5° to 80°. As the samples rotated, the angle θ between the incident beam and normal to the film was varied.

In order to analyze the XRD peak of the blend samples, the XRD diffractograms were deconvoluted using OriginPro 8 to extract the peaks from the scattering circumstantial. In this technique, the baseline correction was used to the specified area. The peaks were than extracted and the area under the graph was calculated. The degree of crystallinity was determined by using the equation below [19]:

$$Xc = \frac{Xcr}{Xcr+Xam} \text{ x } 100\% \quad (6)$$

Where X_{cr} represents the area under the graph of the crystalline scattering and X_{am} is the area under the graph of the amorphous scattering.

Fourier Transform Infrared (FTIR) Analysis

FTIR spectroscopy was used to study the information about the structure of the molecules where the spectra were analyzed to identify the bands attributed to any functional groups. FTIR analysis was carried out using Perkin Elmer spectrophotometer (Model FTIR – Spectrum 400) equipped with Attenuated Total Reflection (ATR). The infrared beam was passed through at the frequency ranged between 4000 and 400 cm^{-1} with resolution of 4 cm^{-1}.

In order to further study the free ions in the polymer electrolyte system, the FTIR spectra were deconvoluted where the Gaussian–Lorentz function was adapted to the Origin Lab software. In the deconvolution technique, FTIR peaks due to dominant ionic movements were selected and the sum of the intensity of all the deconvoluted peaks was ensured to fit the original spectrum [20]. The area under the peaks was determined and the percentage of free ions was calculated using the following equation:

$$\text{Percentage of free ion (\%)}: \frac{A_f}{A_f+A_c} \times 100\% \quad (7)$$

Here, A_f is the area under the peak representing the free ions region and A_c is the total area under the peak representing the contact ions.

RESULTS AND DISCUSSION

Conductivity Studies

Cole-cole plots at ambient temperature are shown in Figure 3. The value of R_b can be determined by the intersection of spike and semicircle line. The semicircles in the plots indicate the characteristic of corresponding combinations of bulk resistance, R_b and bulk capacitance, while the inclined spikes are the capacitance nature of the boundary and absence of electronic conductivity [16].

Electrical conductivity values at room temperature of CS/MC/BMIMTFSI with different amounts of $NH_4CF_3SO_3$ are tabulated in Table 3 and shown in Figure 4. The optimum conductivity was observed at $(7.64 \pm 0.25) \times 10^{-4}$ Scm^{-1} for BPEIL SALT 25. This may be due to the increase in the mobility of NH_4^+ and $CF_3SO_3^-$ ions from the dissociation of the salt. Further addition of $NH_4CF_3SO_3$ into the system had reduced its conductivity. The excess of mobile ions might have the potential to react back and form neutral ion pairs, hence reducing the number of mobile ions. Thus, reduced conductivity was observed [21]. However, further addition of salt was seen to increase the conductivity again (in sample BPEIL SALT 35). This could be due to the dissolution of the polymer in the salt electrolyte (solid polymer in salt electrolyte) due to the higher percentage of salt in the system [23].

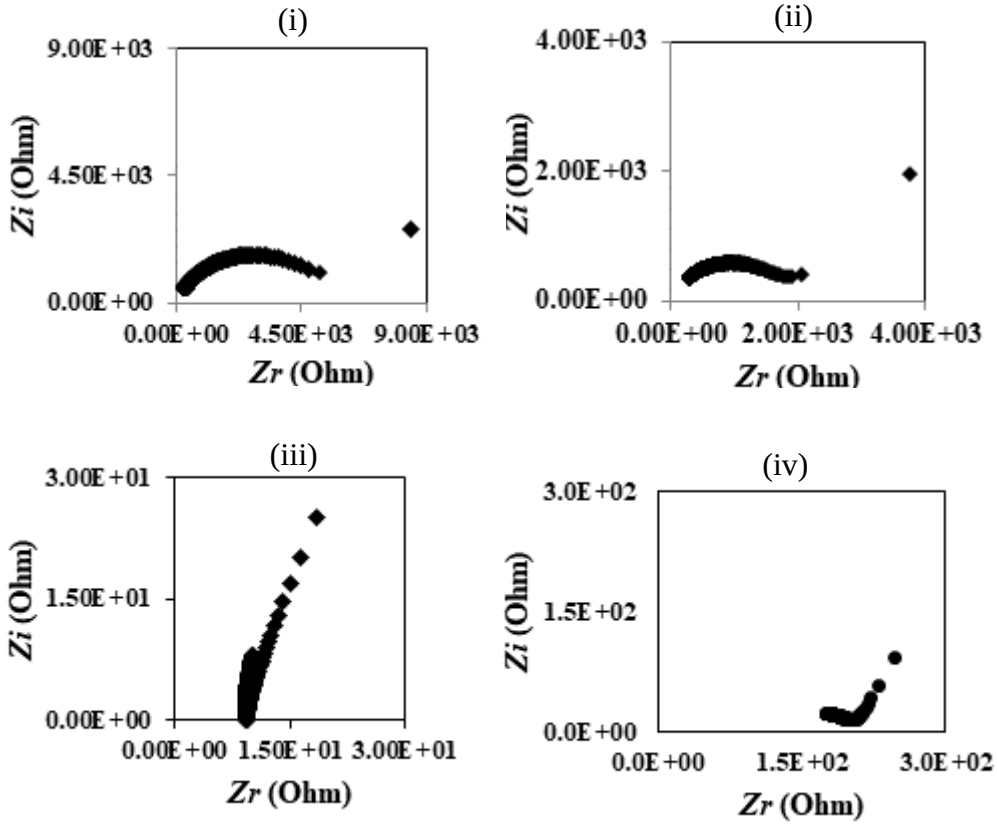

Figure 3. Impedance plots at ambient temperature for (i) BPE IL SALT 10, (ii) BPE IL SALT 15, (iii) BPEIL SALT 25, and (iv) BPEIL SALT 30

Table 3: Conductivity values of all samples as a function of salt concentration

Sample	(Conductivity ± Standard Deviation) / Scm^{-1}
BPE IL Salt 10	$(8.95 \pm 0.02) \times 10^{-7}$
BPE IL Salt 15	$(7.01 \pm 0.12) \times 10^{-8}$
BPE IL Salt 20	$(2.55 \pm 0.09) \times 10^{-6}$
BPE IL Salt 25	$(7.64 \pm 0.25) \times 10^{-4}$
BPE IL Salt 30	$(7.63 \pm 0.41) \times 10^{-6}$
BPE IL Salt 35	$(7.58 \pm 0.20) \times 10^{-5}$
BPE IL Salt 40	$(1.40 \pm 0.13) \times 10^{-6}$

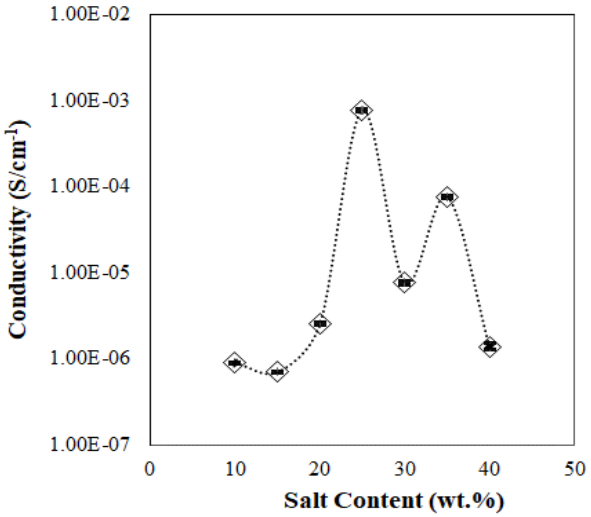

Figure 4. Room temperature conductivity as a function of salt concentration

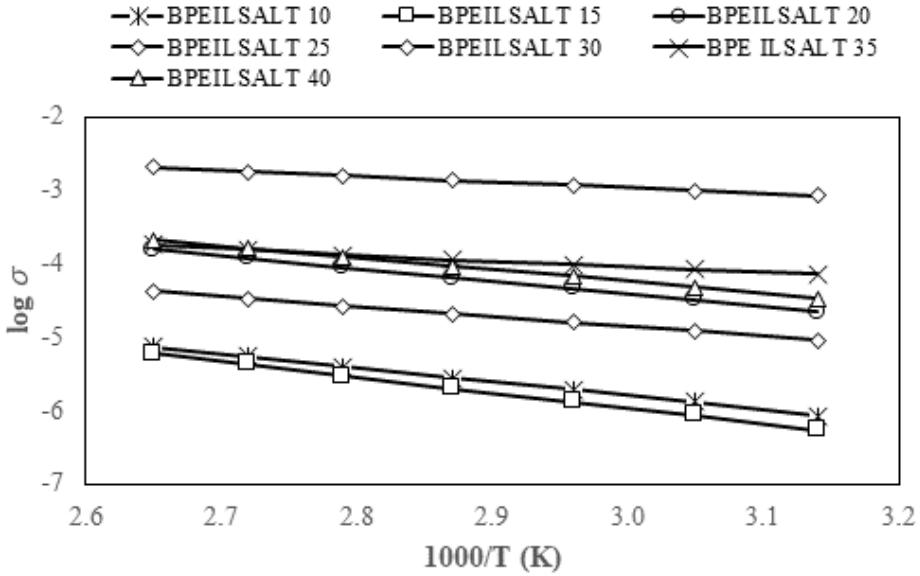

Figure 5. Log conductivity versus 1000/T

The temperature dependence conductivity was plotted, as shown in Figure 5**.** From the graph, it was shown that the conductivity of the samples increased with temperature. This could be explained by the movement of ions in the polymer electrolyte system that could further be enhanced with increasing temperature. Thus, it increased the cation hoping phenomena that hence boosted up the conductivity [3]. The trend of conductivity confirmed the Arrhenius behaviour with regression value (R^2) approaching to unity. The absence of sudden drop in conductivity during temperature increment confirms that ionic conductivity of system is only affected by the presence of charge carriers from the ionic dopant without the influence from the water content [23].

The activation energy, E_a could then be determined from the gradient of the log σ versus 1000/T using the following equation:

$$\sigma = \sigma_o \exp(-E_a)/kT \qquad (8)$$

where σ_o is the pre-exponential factor, E_a is the activation energy, k is the *B*oltzmann constant, and T is the absolute temperature. Figure 6 shows how the activation energy and room temperature conductivity vary as functions of salt concentration. It can be observed that the sample with the maximum conductivity (BPEIL SALT 25) has the lowest activation energy and vice versa. This indicates that the high concentration of dopant salt in electrolyte system can increase ionic conductivity which requires lower energy to migrate greater number of ions in the polymer blend backbone.

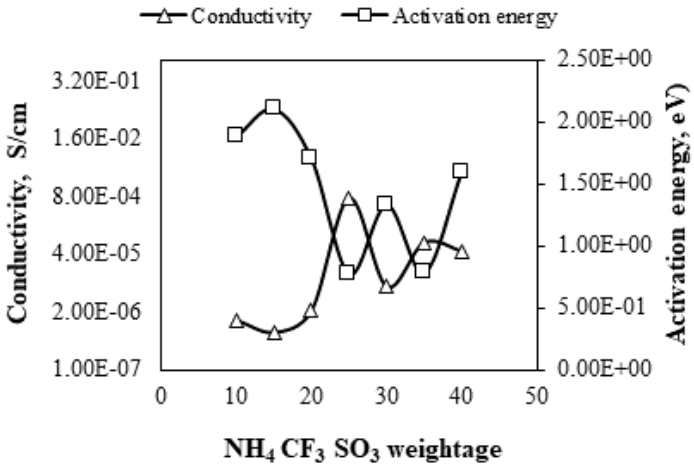

Figure 6. The variation of activation energy, E_a and room temperature conductivity, σ as functions of salt concentration

Ionic conduction mechanism of an electrolyte can be determined by employing Jonscher's universal power law:

$$\sigma(\omega) = A\omega^s + \sigma_{dc} \qquad (9)$$

From Equation (9), since $\sigma_{ac} = A\omega^s$, the value of s can be evaluated from the following equation [24]:

$$\ln \varepsilon_i = \ln A/\varepsilon_o + (s-1)\ln \omega \qquad (10)$$

The value of exponent s is obtained from the slope of the plot $\ln \varepsilon_i$ against $\ln \omega$ as shown in Figure 7. In this study, the acceptable frequency range for CS/MC/BMIMTFSI blend polymer electrolyte was $15.4 < \omega < 15.7$. It could be observed that $\ln \varepsilon_i$ increased with temperature, hence further proved that this system obeyed the Arrhenius behaviour.

Figure 8 displays the graph exponent s versus temperature for sample BPEIL Salt 25. The exponent s was found to be independent of temperature by a small gradient of 0.03. The best model to explain this system is the Quantum Mechanical Tunnelling (QMT) model. In this model it is said that ions tunnel through the potential barrier between the complexation sites [25], where in this study there were several complexation sites that could be present, which were the BMIMTFSI ionic liquid with polymer, NH_4 CF_3 SO_3 salt with polymer, and BMIMTFSI with $NH_4CF_3SO_3$ salt.

XRD Analysis

Figure 9 depicts the XRD spectra for the CS/MC/BMIMTFSI/$NH_4CF_3SO_3$ polymer electrolyte system. It can be observed that after the addition of $NH_4CF_3SO_3$ salt, the peaks became broader. The broadness of the peaks intensified which indicated the amorphousness of the sample. Additionally, the absence of crystalline peaks from $NH_4CF_3SO_3$ salt in the spectra implies that the dissolution of $NH_4CF_3SO_3$ salt in the polymer matrix was complete [26].

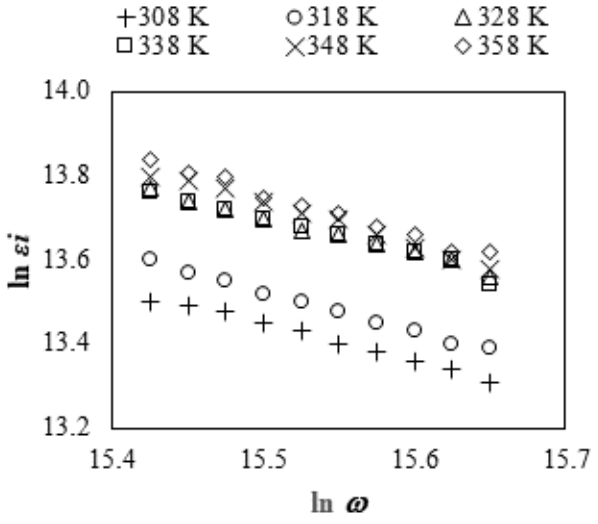

Figure 7. Variation of ln ε_i with frequency at different temperatures

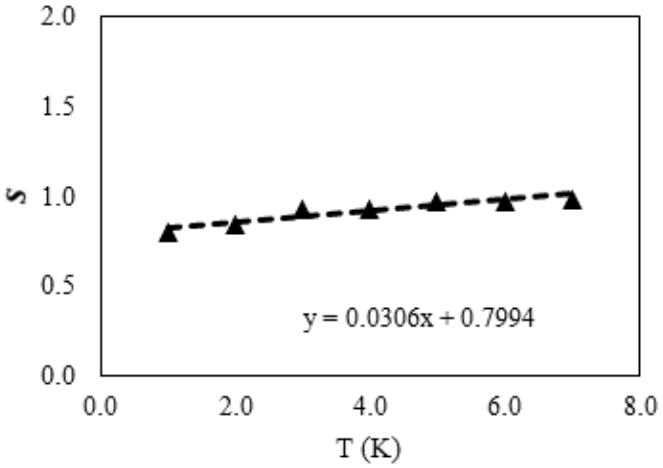

Figure 8. Variation of exponent *s* with temperature

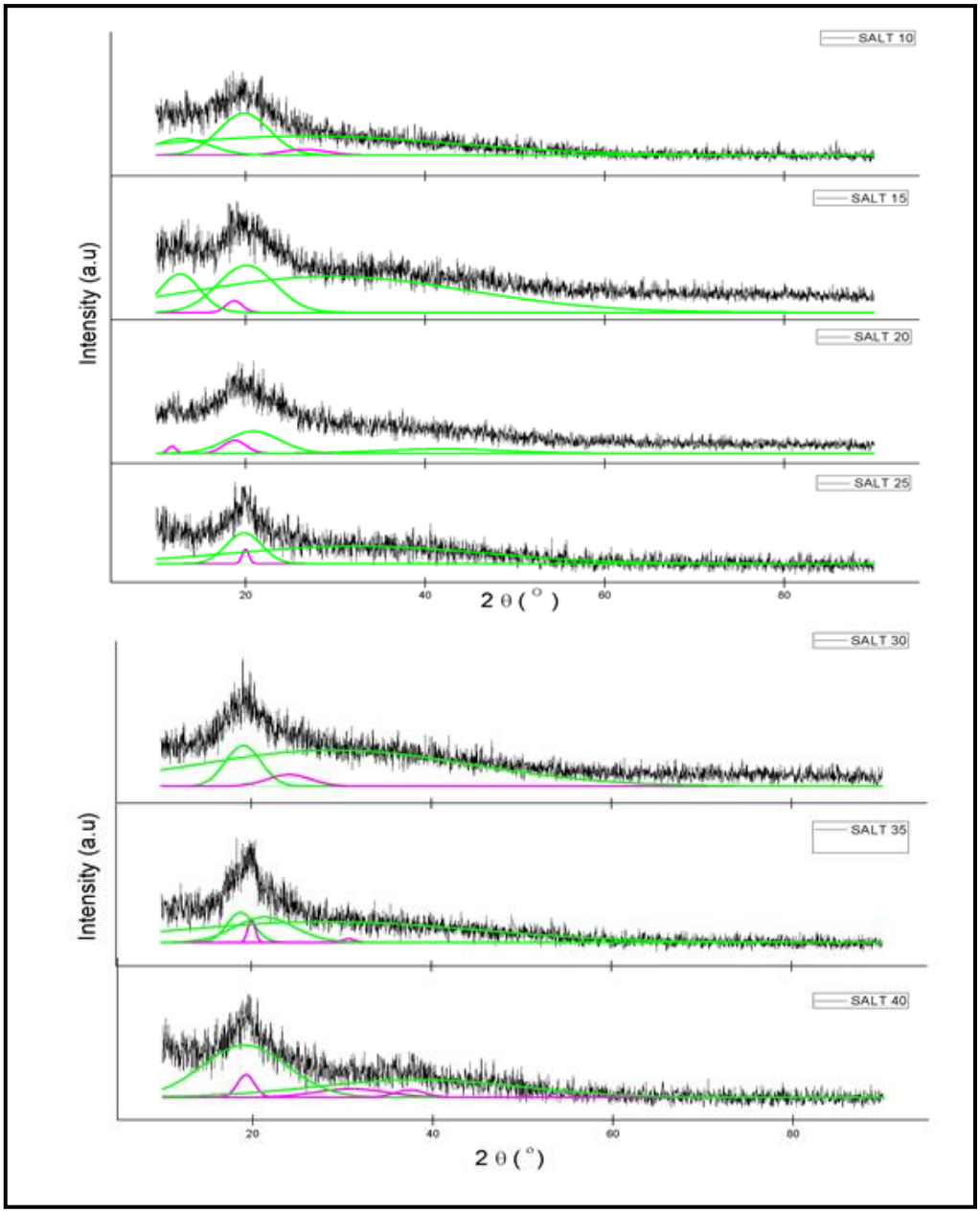

Figure 9. XRD spectra for all BPE IL Salt samples. The green line represents the amorphous hump while the purple line indicates the crystalline peaks.

Table 4. X_c (%) of thin films with the different CS/MC compositions

Sample	Degree of crystallinity, (X_c %)
BPE IL Salt 0	1.91
BPE IL Salt 10	1.89
BPE IL Salt 15	1.77
BPE IL Salt 20	1.73
BPE IL Salt 25	1.53
BPE IL Salt 30	1.79
BPE IL Salt 35	2.01
BPE IL Salt 40	2.23

The degree of crystallinity of the CS/MC/BMIMTFSI/$NH_4CF_3SO_3$ biopolymer electrolyte is tabulated in Table 4. Addition of salt up to 25 wt.% reduced the degree of crystallinity of the samples. This was due to the ordered of polymer host backboned structure had been effectively disturbed by the addition of salt due to possible coordination interaction between H^+ ions from ammonia salt and oxygen atoms from the biopolymer chain. Hence, it increased the amorphous nature of the polymer electrolyte [27].

By determining the degree of crystallinity, the amorphous degree was obtained since the highest crystallinity value corresponds to the lowest amorphous value. The amorphousness of the sample is vital as it provides a greater number of vacant oxygens for hydrogen ions, H^+ to coordinate easily. Thus, the H^+ transportation along the backbone of the electrolyte can be enhanced. The nonstop of H^+ ion mobile along the polymer electrolyte backbone consequently raises the ionic conductivity [28].

FTIR Analysis

Structural changes within the samples were analyzed by FTIR spectroscopy and results are shown in Figures 10 and 11. Different bands were monitored to examine the chemical changes that occurred in the backbone of CS/MC/BMIMTFSI/$NH_4CF_3SO_3$ films.

In Figure 10, the pure $NH_4CF_3SO_3$ spectrum displays four peaks which represent the triflate ion. The peak at 765 cm^{-1} represents the symmetric of CF_3, while the peak at 620 cm^{-1} is attributed to symmetric SO_3 deformation and both peaks at 579 and 515 cm^{-1} are the asymmetric CF_3 deformation and asymmetric SO_3 deformation modes, respectively [29]. These peaks have been found to overlap with the pure MC peaks thus proved that there was an interaction between the triflate ion and MC backbone. According to Mobarak *et al*. [27], as $CF_3SO_3^-$ ion is a negative ion, it will attack an electron deficient atom while NH_4^+ ion, which is a positive ion will interact with electron rich species. Hence the negatively charged

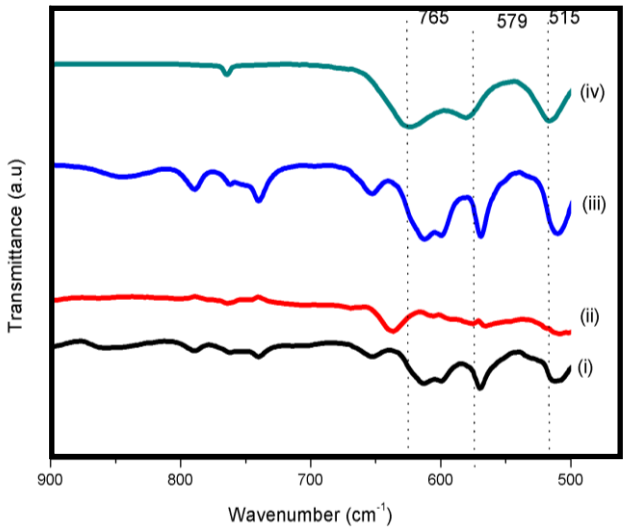

Figure 10. FTIR spectra for (i) BPE IL SALT 0, (ii) BPE IL SALT 25, (iii) pure BMIMTFSI, and (iv) pure $NH_4CF_3SO_3$ at 900 cm^{-1} to 500 cm^{-1}

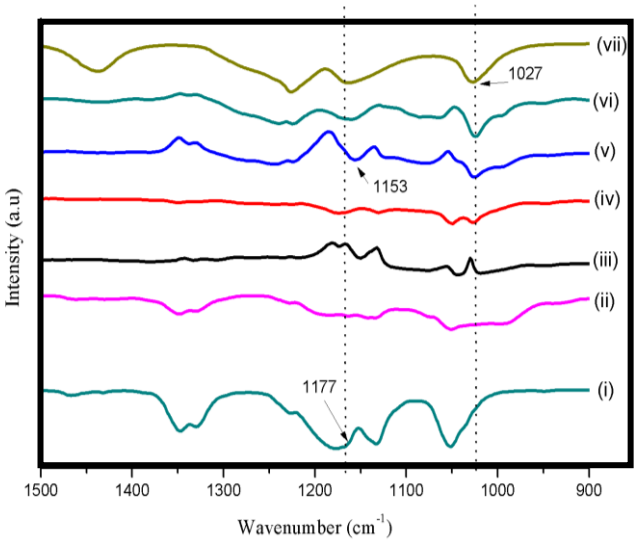

Figure 11. FTIR spectra for (i) pure BMIMTFSI, (ii) BPEIL SALT 0, (iii) BPEIL SALT 10, (vi) BPEIL SALT 15, (v) BPEIL SALT 25, (vi) BPEIL SALT 35, and (vi) pure $NH_4CF_3SO_3$

$CF_3SO_3^-$ ion will interact with carbon from methyl group ($H_3C^{\delta+} - O^{\delta-}$) and NH_4^+ ion will form complexes with oxygen in the MC backbone.

From Figure 11**,** the peak which appeared at 1177 cm^{-1} from pure BMIMTFSI shifted to 1190 cm^{-1}. This observation shows that the imidazolium cation in BMIMTFSI interacted with the oxygen atom from the polymer backbone. Further addition of $NH_4CF_3SO_3$ shifted the peak from 1190 cm^{-1} to 1173cm^{-1}. Thus, it is inferred that the ions from the salt had formed complexation with the functional group from the ionic liquid system.

The peak that appeared at 1027 cm^{-1} in pure $NH_4CF_3SO_3$ represented the stretching of SO_3. A new peak observed at 1027 cm^{-1} indicated the coordination interaction had occurred between (C-O-C) group from the polymer backbone and H^+ from NH_4^+, which is the cation of $NH_4CF_3SO_3$. A similar coordination was found by Shamsudin *et al.* [30].

Figure 12 shows the υ(O-H) peaks at 3420 cm^{-1} which indicated the presence of hydroxyl bands. Two peaks observed at 3190 and 3089 cm^{-1} were attributed to the anti-symmetry stretching of υ(NH_4^+) and symmetry stretching υ(NH_4^+) [31]. The IR spectrum showed that the υ(= C – H) bands of BMIMTFSI ionic liquid had overlapped with the υ(NH_4^+) from the pure $NH_4CF_3SO_3$ and formed two new peaks which were 3214 and 3075 cm^{-1}. Thus, it could be concluded that the hydrogen (H) atom from the υ(NH_4^+) had directly attached to the carbon of imidazolium from BMIMTFSI ionic liquid. Additionally, a hydroxyl band was observed at 3300 cm^{-1} for BPEIL Salt 0. Upon addition of $NH_4CF_3SO_3$ salt, the band shifted to

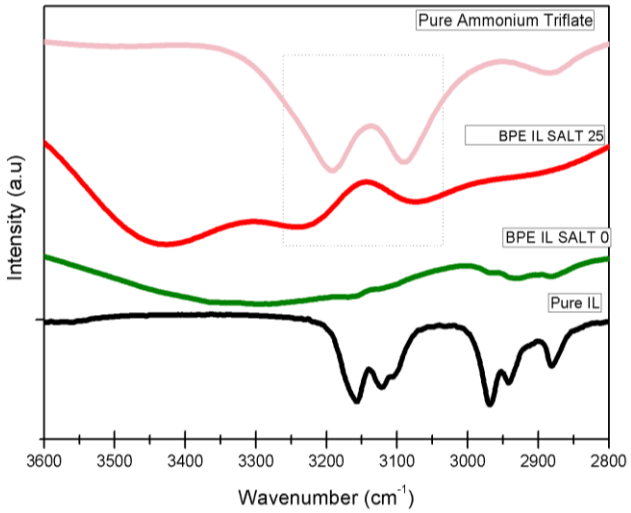

Figure 12. FTIR spectra for BPE IL SALT (i) 0 (i) and (ii) 25, (iii) pure BMIMTFSI, and (iv) pure $NH_4CF_3SO_3$ at 3600 cm^{-1} to 2800 cm^{-1}

3400 cm^{-1}, which indicated the interaction between the hydroxyl bands with $NH_4CF_3SO_3$. According to Hema *et al*. [32], during the addition of salt into the polymer host, the cation is expected to coordinate within the polymer host backbone which can affect the structure of the polymer and influence certain infrared active modes of vibration. This is also another evidence of complexation between the cation from the salt and hydroxyl group from the polymer backbone [33].

In order to determine the presence of free ions, ion pairs and highly aggregated ions in the polymer blend – ionic liquid - salt complexes, deconvolution of the IR spectra of the samples was carried out in the symmetric $\upsilon(-NH_4)$ stretching region as shown in Figure 13. The IR curve fitting bands at 3150 cm^{-1} to 3300 cm^{-1} in the polymer blend–ionic liquid - salt complexes showed the presence of different ionic species of ammonium anions.

Table 5 lists the percentage of free ions and contact ions of CS/MC/BMIMTFSI/$NH_4CF_3SO_3$ polymer electrolytes. The percentage of free ions increased with the addition of $NH_4CF_3SO_3$ salt. However, beyond 25 wt.% of salt, the percentage of free ions reduced. This observation inferred that the excess free ions would recombine with each other and form neutral ions.

Table 5. Percentages of free ions and contact ions for chitosan/methyl cellulose/ BMIMTFSI/ $NH_4CF_3SO_3$ biopolymer electrolyte

Sample	Free Ion %	Contact Ion %
BPEIL Salt 10	28.1	71.9
BPEIL Salt 15	32.3	67.7
BPEIL Salt 20	35.4	64.6
BPEIL Salt 25	49.7	50.3
BPEIL Salt 30	41.1	68.9
BPEIL Salt 35	40.7	59.3
BPEIL Salt 40	39.5	60.5

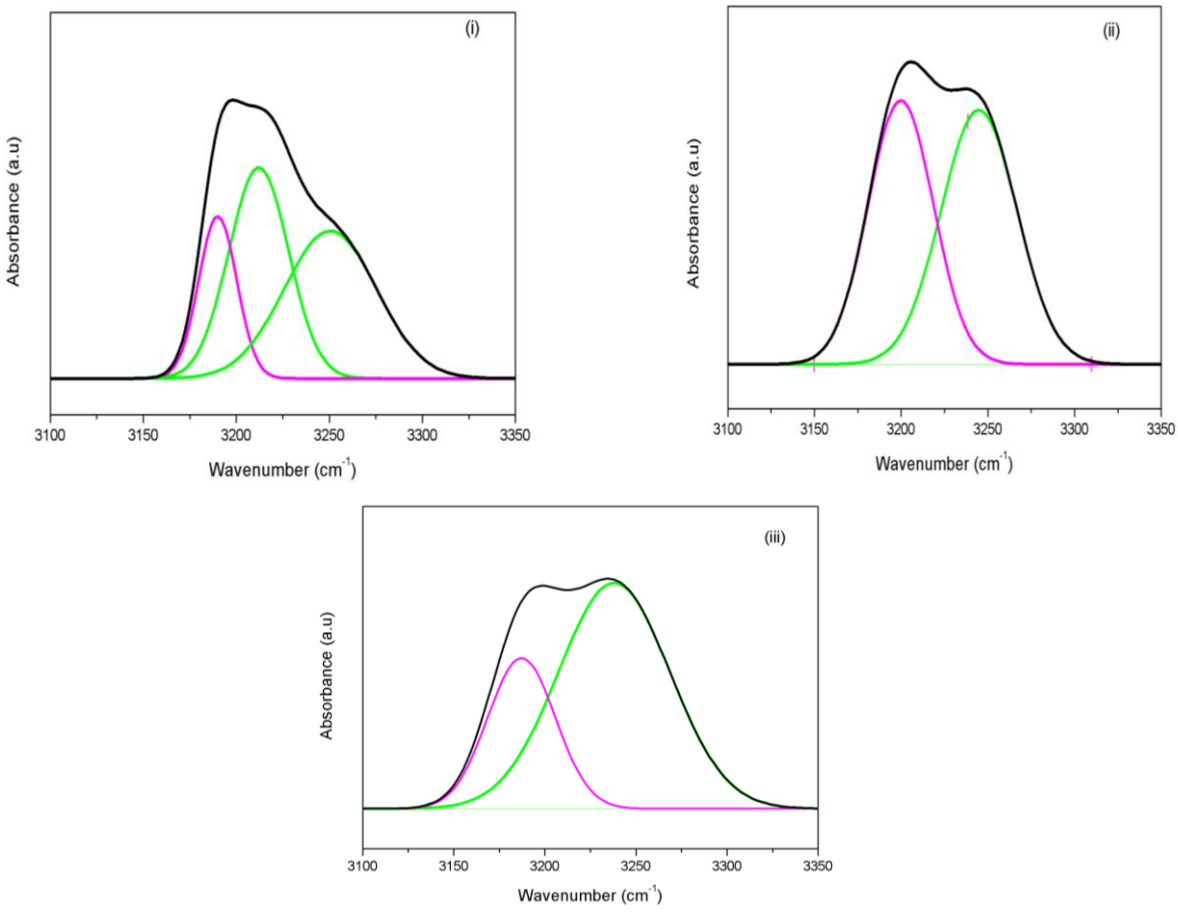

Figure 13. Deconvolution of FTIR spectra for (i) BPEIL Salt 20, (ii) BPEIL Salt 25, and (iii) BPEIL Salt 40. The purple spectra indicate the free ions while the green spectra for the contact ions.

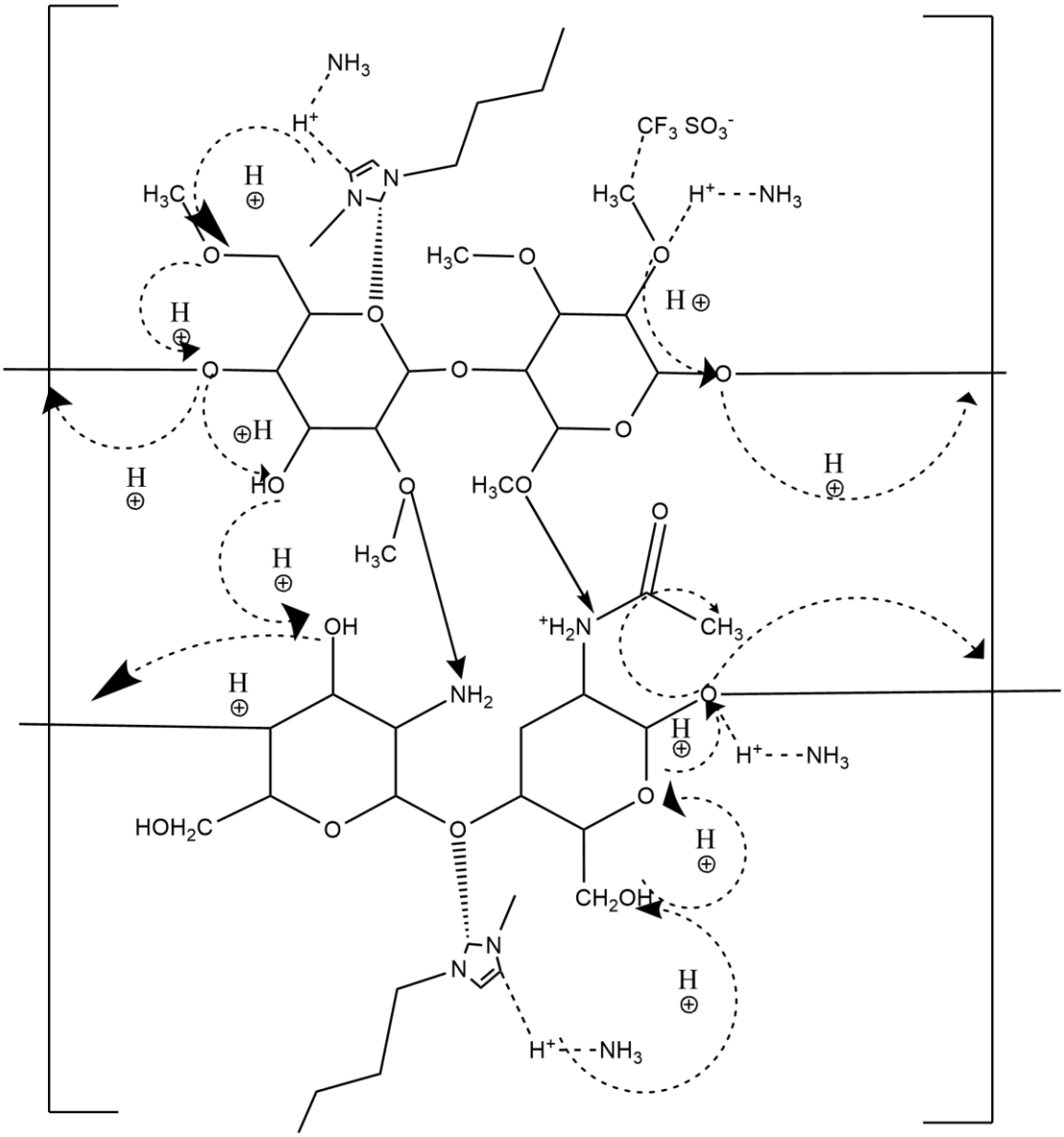

Figure 14. The proposed chemical interaction mechanism of CS/MC/BMIMTSI/ $NH_4CF_3SO_3$ polymer electrolyte

A chemical interaction mechanism between the blended polymers (CS/MC), ionic liquid (BMIMTFSI) and salt ($NH_4CF_3SO_3$) has been proposed as illustrated in Figure 14. From the figure, the conducting species in the system is H^+. Although there were three more possible conducting cation in the system, which were $BMIM^+$, NH_3^+ and NH_4^+, conduction from H^+ ion was more likely to occur in the polymer-ammonium salt system [34]. The interactions in the present system occurred through the exchange of ions between sites and can be explained by Grotthus mechanism. Ammonium salt consists of four hydrogen atoms which two of them are bound identically. The other two hydrogen atoms are either strictly or weakly bound. The weakly bound H^+ ion can be easily dissociated and may hop from one site to another, leaving a vacancy. This vacancy will be filled by another H^+ ion from a neighbouring site. Thus, the hydrogen ion in NH_4^+ from the $NH_4CF_3SO_3$ is presumed to interact with the oxygen at the coordinating site of the host polymer (CS/MC) as proposed.

CONCLUSION

The highest conductivity obtained was 7.64×10^{-4} S cm^{-1} at ambient for the sample containing 25 w.t% $NH_4CF_3SO_3$. The increase in conductivity could be attributed to the increase in the number of free mobile ions. However, the excess of mobile ions would shortened the distance of two free ions and increased the probability of the free ions to reassociate and become neutral, hence reduced conductivity. Temperature helps to assist ion movement and provides an alternative pathway for the cation hoping, hence boosts conductivity. From the plot log σ versus 1000/T, the polymer electrolyte obeyed Arrhenius behaviour. The activation energy varied with

conductivity where the highest conducting sample had the lowest E_a of 0.7732 eV. QMT model was used to describe the conduction mechanism in this present study. XRD results related the amorphous nature to conductivity while FTIR analyses showed that interaction had occurred in the complexes.

ACKNOWLEDGEMENT

This work was funded by FRGS under vote USIM/FRGS-FST-32-51312. The authors would like to thank Faculty of Science and Technology, Universiti Sains Islam Malaysia and School of Fundamental Science, Universiti Malaysia Terengganu for the facilities provided.

REFERENCES

1. Rudhziah S., A. Ahmad, I. Ahmad, N.S. Mohamed (2015) Biopolymer Electrolytes Based on Blend of Kappa-Carrageenan and Cellulose Derivatives for Potential Application in Dye Sensitized Solar Cell. *Electrochimica Acta*, **175**, 162–168.

2. Campo V. L., D. F. Kawano, D. Braz, I. Carvalho (2009) Carrageenans: Biological Properties, Chemical Modifications and Structural Analysis. *Carbohydrate Polymer*, **77**, 167–180.

3. Misenan M. S. M., Isa M. I. N., and Khiar A. S. A. (2018) Electrical and structural studies of polymer electrolyte based on chitosan/methyl cellulose blend doped with BMIMTFSI. *Material Research Express*, **5(5)**, 55304.

4. Arifin N. A. and Khiar A. S. A. (2015) Effect of BMITFSI to the electrical properties of methylcellulose/chitosan/NH_4TF-based polymer electrolyte. *Proc. of SPIE*, **9668**, 96681J.

5. Yusof Y. M., Illias H. A., Shukur M. F. and Kadir M. F. Z. (2017) Characterization of starch-chitosan blend-based electrolyte doped with ammonium iodide for application in proton batteries. *Ionics*, **23(3)**, 681–697.

6. Hu, Q., Caputo, A and Sadoway, D.R (2013) Solid-state Graft Copolymer Electrolytes for Lithium Battery Applications, *Journal of Visualized Experiments*, **78**, 4–6.

7. Chai M. N. and M. I. N. Isa (2015) Structural Study of Plasticized Carboxy Methylcellulose Based Solid Biopolymer Electrolyte. *Advanced Material Research*, **1107(18)**, 242–246.

8. Sudhakar Y. N. and M. Selvakumar (2012) Lithium perchlorate doped plasticized chitosan and starch blend as biodegradable polymer electrolyte for supercapacitors. *Electrochimica Acta*, **78**, 398–405.

9. Shukur, M. F. R. Ithnin, H. A. Illias and M. F. Z. Kadir (2013) Proton conducting polymer electrolyte based on plasticized chitosan-PEO blend and application in electrochemical devices. *Optical Material*, **35 (10)**, 1834–1841.

10. Jung, Y. C., Seul-Ki Kim, Moon-Sung Kim, Jeong-Hye Lee, Man-Seok Han, Duck-Hyun Kim, Woo-Cheol Shin, Makoto Ue, Dong-Won Kim (2015) Ceramic separators based on Li^+-conducting inorganic electrolyte for high-performance lithium-ion batteries with enhanced safety. *Journal of Power Sources*, **293**, 675–683.

11. Khiar A. S. A. and A. K. Arof (2011) Electrical Properties of Starch/Chitosan-NH_4 NO_3 Polymer Electrolyte. *WASET*, **5(3)**, 23–27.

12. Misenan, M. S. M, Ali, E. S, Khiar, A. S. A. (2018) Conductivity, dielectric and modulus study of chitosan-methyl cellulose–BMIMTFSI polymer electrolyte doped with cellulose nano crystal. *AIP Conference Proceedings*, **1972(1)**, 030010.

13. Buraidah M. H. and Arof, A. K. (2011) Characterization of chitosan/PVA blended electrolyte doped with NH 4I. *Journal of Non Crysttaline Solids*, **357(16–17)**, 3261–3266.

14. Hafiza M. N. and Isa, M. I. N (2014) Ionic Conductivity and Conduction Mechanism Studies of CMC/Chitosan Biopolymer Blend Electrolytes. *Earth Sciences Research Journal*, **3(11)**, 50–56.

15. Buraidah, M. H., Teo, L. P., Au Yong, C. M., Shah, S. and Arof, A. K. (2016) Performance of polymer electrolyte based on chitosan blended with poly(ethylene oxide) for plasmonic dye-sensitized solar cell, *Optical Materials*, **57**, 202–211.

16. Navaratnam S., K. Ramesh S. Ramesh A. Sanusi W.J. Basirun A. K. Arof (2015) Transport Mechanism Studies of Chitosan Electrolyte Systems. *Electrochimica Acta*, **175**, 68–73.

17. Pinotti A., M. A. Garcı´, M. N. Martino, N. E. Zaritzky (2007) Study on Microstructure and Physical Properties of Composite Films Based on Chitosan and Methylcellulose. *Food Hydrocolloids*, **21**, 66–72.

18. He, Y., Zhu, B., Inoue, Y. (2004) Hydrogen Bonds in Polymer Blends. *Progress in Polymer Science*, **29**, 1021–1051.

19. Garcı´a M. A., A. Pinotti, M. Martino, N. Zaritzky (2009) Electrically treated composite

films based on chitosan and methylcellulose blends. *Food Hydrocolloids*, **23**, 722–728.

20. Chai, M. N. & M. I. N. Isa (2016) Novel Proton Conducting Solid Bio-polymer Electrolytes Based on Carboxy methyl Cellulose doped with Oleic Acid and Plasticized with Glycerol. *Scientific Report Nature*, **6**, 27328.

21. Dzulkurnain, N. A., M. S. A. Rani, A. Ahmad and N. S. Mohamed (2018) Effect of lithium salt on physicochemical properties of P(MMA-co-EMA) based copolymer electrolytes for dye-sensitized solar cell application. *Ionics*, **24(1)**, 269–279.

22. Wu, B., Wang, L., Li, Z., Zhao, M., Kaihao, C., Liu, S., Pu, Y., Li, J. (2016) Performance of "Polymer-in-Salt" Electrolyte PAN-LiTFSI Enhanced by Graphene Oxide Filler. *Journal of The Electrochemical Society*, **163**, A2248–A2252.

23. Hafiza M. N. and M. I. N. Isa (2017) Solid polymer electrolyte production from 2-hydroxyethyl cellulose: Effect of ammonium nitrate composition on its structural properties. *Carbohydrate Polymer*, **165(3)**, 123–131.

24. Samsudin A. S., M. I. A. Aziz, M. I. N. Isa (2012) Natural Polymer Electrolyte System based on Sago: Structural and Transport Behaviour Characteristics. *International Journal of Polymer Analysis and Characterization*, **17**, 600–607.

25. Majid S. R. and A. K. Arof (2007) Electrical behaviour of proton-conducting chitosan-phosphoric acid-based electrolytes. *Physica B*, **390**, 209–215.

26. Singh, R., N. A. Jadhav, S. Majumder, B. Bhattacharya and P. K. Singh (2013) Novel biopolymer gel electrolyte for dye-sensitized solar cell application. *Carbohydrate Polymer*, **91(2)**, 682–685.

27. Mobarak N. N, N. Ramli, M. P. Abdullah and A. Ahmad (2013) Spectroscopic studies of carboxy methyl chitosan-ammonium triflate ($NH_4CF_3SO_3$) based solid polymer electrolytes. *AIP Conference Proceedings*, **1571**, 843.

28. Liew, C., S. Ramesh and A. K. Arof (2013) A novel approach on ionic liquid-based poly (vinyl alcohol) proton conductive polymer electrolytes for fuel cell applications. *International Journal of Hydrogen Energy*, **39(6)**, 2917–2928.

29. Khiar, A. S. A., R. Puteh and A. K. Arof (2006) Characterizations of chitosan-ammonium triflate ($NH_4CF_3SO_3$) complexes by FTIR and impedance spectroscopy. *Physica Status Solidi A*, **203(3)**, 534–543.

30. Samsudin, A. S. Khairul, W. M. and Isa, M. I. N. (201) Characterization on the potential of carboxy methylcellulose for application as proton conducting biopolymer electrolytes. *International Journal of Polymer Analysis and Characterization*, **358**, 1104–1112.

31. Mobarak N. N., A. Ahmad, M. P. Abdullah, N. Ramli, M. Y. A. Rahman (2013) Conductivity enhancement via chemical modification of chitosan based green polymer electrolyte. *Electrochimica Acta*, **92**, 161–167.

32. Hema, M., Selvasekarapandian, S., Arunkumar, D., Sakunthala, A. and Nithya, H. (2009) FTIR, XRD and ac impedance spectroscopic study on PVA based polymer electrolyte doped with NH_4X (X = Cl, Br, I). *Journal of Non-Crystalline Solids*, **355(2)**, 84–90.

33. Kadir, M. F. Z., Majid, S. R. and Arof, A. K. (2010) Plasticized chitosan – PVA blend polymer electrolyte-based proton battery. *Electrochimica Acta*, **55(3)**, 1475–1482.

34. Ramlli M. A., Kamarudin, K. H. and Isa, M. I. N. (2015) Ionic Conductivity and Structural Analysis of Carboxymethyl Cellulose Doped with Ammonium Fluoride as Solid Biopolymer Electrolytes. *American-Eurasian Journal of Sustainable Agriculture*, **9(2)**, 46–51.